Published in final edited form as:
Langmuir. 2011 January 4; 27(1): 494–498. doi:10.1021/la104085t.

Isoelectric Focusing in a Drop

Noah G. Weiss[1], **Mark A. Hayes**[1], **Antonio A. Garcia**[2,*], and **Rafat R. Ansari**[3]

[1] Department of Chemistry and Biochemistry, Arizona State University, Tempe, AZ

[2] School of Biological and Health Systems Engineering, Arizona State University, Tempe, AZ

[3] NASA Glenn Research Center, Cleveland, OH

Abstract

A novel approach to molecular separations is investigated using a technique termed droplet-based isoelectric focusing. Drops are manipulated discretely on a superhydrophobic surface, subjected to low voltages for isoelectric focusing, and split—resulting in a preparative separation. A universal indicator dye demonstrates the generation of stable, reversible pH gradients (3–10) in ampholyte buffers and these gradients lead to protein focusing within the drop length. Focusing was visually characterized, spectroscopically verified, and assessed quantitatively by non-invasive light scattering measurements. It was found to correlate with a quantitative model based on 1D steady state theory. This work illustrates that molecular separations can be deployed within a single open drop and the differential fractions can be separated into new discrete liquid elements.

Introduction

Separating molecules in a complex mixture is often a vital treatment for chemical and biological analyses. There exist needs for both low-resolution separations, used for simplifying samples, as well as high-resolution separations, where pure molecular fractions are isolated from others. Moreover, devices that perform these separations with low-volume sample size are of growing interest. Miniaturized devices that address these needs can provide lower cost, higher productivity, and more effective decision-making. The miniaturization of this technology (along with other design elements) allows it to be broadly deployed to the sampling locations, rather than the current paradigm of transportation to a central laboratory with complex and expensive instrumentation. Various microfluidic systems have been developed in this vein over the past ten years.[1–6]

Microfluidic systems can be categorized either as flow, digital, or hybrid depending upon whether the fluid of interest is fed continuously through microchannels, moved as discrete drops, or is manipulated as discrete drops within a continuous immiscible liquid, respectively.[7] In any case, the ability to conduct molecular separations of complex samples is a desirable feature of such microfluidic systems. Flow and hybrid systems typically require the use of microchannels which can create some challenges. These range from difficult integration of sample pre-processing and surface fouling to channel blockages resulting from bubbles or particulates. Digital microfluidic systems overcome most of these obstacles by allowing discrete fluidic processing in open environments and minimizing surface area contact. Perhaps the most daunting challenge in the digital system, however, is the implementation of a molecular separation step.[8]

[*]Professor Antonio Garcia, Arizona State University, PO Box 879709, Tempe, AZ 85287-9709, 480-965-8798 (phone), 480-727-7624 (fax), tony.garcia@asu.edu.

A few strategies for performing separations within drops have been explored recently. Electrophoretic[9] and dielectrophoretic[10,11] forces were exploited to create binary separations of particles 1–10 μm which increased their concentration about two-fold. Methods for collecting magnetic particles[12,13] and for extracting proteins by precipitation[14] have also been developed in drops. In an alternative approach, a microchannel based separation was integrated onto a digital platform.[15] Although such sophisticated efforts open up new opportunities for digital microfluidics, we are interested in exploring a separation mechanism which could separate more than two analytes and be carried out in the digital state. Such a separation would maintain simplicity, avoid unwanted effects of microchannels, and be capable of integrating into any digital microfluidic platform regardless of actuation method (electric[8] or magnetic[16]). Here we explore the idea of performing a molecular separation within an open drop using droplet-based isoelectric focusing (dIEF).

Isoelectric focusing, traditionally carried out in gels and more recently capillaries,[17,18] is a type of gradient separation which separates molecules based on their isoelectric point (pI) or pH of net neutral charge. A uniform electric field and a pH gradient are applied along the separation length which causes molecules to focus in the region of net neutrality which is specific to their chemical composition. The term focusing comes from the fact that diffusion is counter-balanced by electrophoresis once a steady state is reached. A molecule that diffuses out of the neutral zone towards the anode (lower pH region) will assume a positive charge and migrate back towards the focus point and vice versa if it diffuses towards the cathode. Thus, the steady state concentration distribution of a 1D system is given by the following:[19]

$$C(x)=C_o e^{\frac{-\left(\rho E(x-x_{pI})^2\right)}{2D}} \quad (1)$$

where C is the concentration of a component, C_o is the concentration maximum, $\rho=d\mu/dx$ is the slope of the electrophoretic mobility (μ): assumed to be constant within the focused zone, E is the electric field strength, x is the coordinate along the direction of current, x_{pI} is the isoelectric point, and D is the diffusion coefficient. This is a Gaussian concentration profile with standard deviation given by:

$$x_\sigma = \pm \sqrt{\frac{D}{\rho E}} \quad (2)$$

Eqs (1–2) are insightful because they identify the important parameters for generating narrow bands of material and can be used to model more complex systems. Proteins are particularly well suited for IEF because they have large mobility slopes (ρ) and small diffusion coefficients (D). Applying these concepts within an open drop gives rise to the technique of dIEF.

In addition to visualization, non-invasive light scattering measurements are used to confirm protein focusing in dIEF. Dynamic light scattering (DLS) was originally developed to study the fluid dispersions of colloidal (size ≤1 μm) particles.[20] The ability of DLS to detect early changes in the molecular morphology of proteins has the potential to help develop new treatments to combat various ocular and systemic diseases prior to the onset of irreversible changes.[21] In a DLS experiment, a constantly fluctuating speckle pattern is seen in the far field when light passes through an ensemble of small particles suspended in a fluid.[20] This speckle pattern is the result of interference in the light paths and it fluctuates as the particles

in the scattering medium perform random movements on a time scale of ≥1 μs due to the collisions between themselves and the fluid molecules (Brownian motion). In the absence of particle-particle interactions (dilute dispersions) light scattered from small particles fluctuates rapidly while light scattered from large particles fluctuates more slowly. Generally speaking, an increase in particle sizes (from nanometers to a few microns) and an increase in the number or density of these particles result in an increase in total scattered light intensity (static light scattering). The experiments reported here utilize this feature.

Superhydrophobic surfaces (SHS) provide some unique opportunities for manipulating fluids in the digital state,[22–25] and much progress has been made in fabrication over the years.[26,27] An important realization is that aqueous drops take up well-defined shapes and do not spread on a SHS. Thus, if manipulated properly the drop can be positioned and stabilized in shapes necessary for carrying out a separation without the need for a supporting chamber (e.g., channel, capillary, etc.). With the interest of developing low cost, simple devices we utilize a roughened polyethylene SHS to allow manipulation of drops.[16,28,29] This paper presents a preliminary yet detailed study of the dIEF principles. Through this work we demonstrate the generation of stable pH gradients, well behaved protein focusing, and accurate quantitative modeling. These findings suggest that dIEF could be applied for sample purification of complex biological mixtures or integration into digital microfluidic devices.

Experimental Methods

Chemicals and Materials

Unless mentioned otherwise all chemicals and materials were obtained from Sigma-Aldrich (St. Louis, MO, USA). Pharmalyte brand ampholyte (pH 3–10) was obtained from Amersham Biosciences (Postcataway, NJ, USA). A stock universal indicator solution was prepared with 400 ppm phenolphthalein, 50 ppm thymol blue, 300 ppm bromothymol blue, and 150 ppm methyl red in 10% ethanol (v/v). Electrodes were made from 0.5 mm diameter platinum wire which was shaped into 5 mm diameter loops. A digital power supply was used for applying voltages and measuring current (SMU2064, Signametrics, Seattle WA). Superhydrophobic polyethylene surfaces were prepared as previously described.[16] Briefly, low density polyethylene was dissolved in xylene and methyl ethyl ketone (a non-solvent) was sequentially added. The mixture was allowed to slowly crystallize on a polyethylene substrate by slow heating and evaporation creating a roughened surface. A USB camera (MiniVid, LW Scientific, Lawernceville GA) was used to capture all movies and images of the dIEF experiments.

Digital Isoelectric Focusing

For pH gradient visualization the samples contained 2 % (w/v) ampholyte pH 3–10 and 10 % (v/v) stock universal indicator. For preliminary protein studies the samples contained 2 % (w/v) ampholyte pH 3–10 and 0.25 mg/mL myoglobin. Drops ranging in volume from 50–200 μL were pinned and stretched 0.5–2 cm between two loop electrodes on a superhydrophobic surface (Figure 1). This led to drops with an allantoidal shape where the drop body is cylindrical with rounded ends where it pinned to the electrodes. Depending on the experiment, a low voltage was applied ranging from 5–30 V resulting in currents 0.1–1 mA. Voltages were applied for durations up to an hour. Over this period the current decreased to about 40% of its initial value; a result typical of a loss of charge carriers in IEF. The nominal electric field strength is estimated by dividing the applied voltage by the drop length. Video footage was collected to characterize pH gradient formation. For protein separation experiments, the drop was split as described below.

Drop Splitting and Protein Quantification

Drops were split using a thin superhydrophobic substrate to penetrate and separate the drop into two. Initially, this surface was mounted on a slide positioned above the drop (Figure 1). When the dIEF experiment was complete the slide was lowered splitting the drop into two sections. This action is capable of physically splitting a water drop to generate two new daughter drops. When proteins or other surfactants are present, the superhydrophobic surface becomes wettable and the drop no longer has the necessary surface energy to independently form two new drops. Nonetheless, the penetrated surface provides a barrier to separately collect the split portions without mixing. Thus, after lowering the superhydrophobic 'guillotine' in these experiments the two separated portions were collected by pipette, weighed to determine volume, and stored for quantification.

Myoglobin was quantified by absorbance measurements (λ = 405 nm, ε_{405nm} = 245,000 M^{-1} cm^{-1}) using a small-volume flow-cell built in house. This consisted of a 320 μm internal diameter capillary threaded into a CE flow cell with fiber optics delivering light from a DH-2000 deuterium lamp to a USB 4000 bench top spectrometer (Ocean Optics, Dunendin, FL, USA). This apparatus only requires 15 μL of sample while providing a reasonable path length and is well suited for quantifying the <100 μL fractions collected after drop splitting.

Light Scattering Detection of dIEF

A compact fiber-optic light scattering probe was used to measure aggregation in the protein sample as the DC voltage was applied (Figure 2). It was mounted roughly 5 cm from the drop surface and scanned laterally across the length of the drop at a rate of 50 μm/s using a programmable stage motor. The total time to collect a single scan (6 mm length) was 2 minutes. Allowing time for the probe to return to its starting position, scans were collected every 2.5 minutes for the duration of the dIEF experiment. To successfully capture the progression, light scattering intensity was continuously recorded for the entire experiment duration. The setup comprises a semiconductor laser (λ=639.4 nm, power=80 μW), a photodetector (avalanche photodiode based photon counting module), a DLS probe built at NASA for both static and dynamic light scattering configurations (scattering angle=163.0 degrees, focal length=16 mm, scattering volume ~50 μm^3), a translation stage with a motorized actuator, for accurate positioning, (to which the DLS fiber optic probe is mounted on a multi axis translation stage), and a Pentium based computer containing a digital correlator card (BI-9000) for data acquisition. This system has been previously used in protein crystal growth experiments,[30] particle sizing applications in flowing dispersions,[31] in protein characterization of ocular tissues in live animals,[32] and in clinical ophthalmic applications for the early detection of cataract.[33] Only the static (total intensity) light scattering measurements were made in the experiments reported here.

Results and Discussion

pH Gradient Formation

Electrolytic pH gradient generation has been demonstrated theoretically and experimentally for microfluidic systems,[34,35] and we hypothesized a similar process could take place within open drops. It is based on the principle of oxidizing water at the anode to form H^+ ions and reducing water at the cathode to form OH^- ions. As time evolves, these ions can be transported throughout the solution through diffusion, electromigration, fluid flow, and exchange with buffering ions. Thus, a pH profile can develop across the solution and dynamically change until reaching an equilibrium state defined by the solution and electrical properties. Buffering of the solution has a critical role in generating smooth, stable gradients since electrolysis of non-buffered solutions typically leads to a step-like pH profiles across the system length.[36] Therefore, the first phase of experimentation was to examine the

possibility of forming smooth, stable pH gradients by electrolyzing water in drops after positioning and stretching them on a SHS.

A universal indicator dye sensitive to a pH range of 3–10 was used for visual characterization of gradient formation (Figure 3i). Not surprisingly, when 25 mM phosphate is used step-like pH profiles develop rather than uniform gradients (data not shown). In these experiments, extreme pH zones slowly evolve over time from the electrodes, pH<3 for the anode and pH>10 for the cathode, until a very narrow pH transition region remains. This pH profile is likely formed because the rate of electrolysis exceeds mass transport and exchange with buffering ions (i.e., source exceeds sink). Next, a common IEF ampholyte mixture (Pharmalyte pH 3–10) was used and this generated stable, uniform pH gradients as indicated by the color profile of the dye. Still images show the formation of a pH gradient ranging from pH ~ 4 (light red, anode side) to pH ~ 9 (blue, cathode side) (Figure 3a–d). The gradient was formed in about 10 minutes and was found to be stable over longer periods of applied voltage (at least 45 minutes). This is an indication that the ampholyte buffers are distributed across the drop such that they buffer the pH and efficiently transport the continual generation of H^+ and OH^- ions. The pH gradient was reversed by switching electrode polarity (Figure 3e–h). It took about 15 minutes for the gradient to reverse, but similarly a stable profile was observed over prolonged applications of voltage. For comparison, reference pH solutions and their universal indicator color response are shown (Figure 3i).

Traditional IEF theory predicts individual ampholyte species will focus into steady state zones, stacked in order of pIs, and will control local pH.[37] Experimental investigations have demonstrated that ampholytes are often distributed in a much more random fashion.[38] Thus, it is uncertain how ampholyte components are distributed in these drop experiments. An exponential reduction in current is observed over time characteristic of a decrease in conductivity from ampholyte focusing. Overall these results demonstrate that pH gradients within drops can be generated, held stable with appropriate buffers, and reversed by switching polarity.

Characterizing Protein Focusing in dIEF

The next phase of experiments involved characterizing the dIEF focusing behavior of a single protein and comparing the results to 1D steady state theory. Myoglobin (pI 7.2) was selected as a target since it has a chromophore allowing easy detection and its IEF properties were previously studied.[39] Assuming a linear pH gradient and defining the anode as pH 3 at x=0 and the cathode as pH 10 at x=1.5 cm means that myoglobin would focus at x_{pI}=0.9 cm. Several trials were conducted where 5–20 V was applied across 150 μL drops for twenty minutes. Subsequently, the drops were split at an average position of x=0.7 cm and the protein content in the two resultant droplets, defined as anode and cathode droplets, was quantified by absorbance measurements.

Two clear observations arose from these experiments (Table 1). The first is that the protein became more isolated to the cathode droplet side with increasing electric field. This is an expected result since bandwidth becomes narrower with increasing field (Eq (2)) and myoglobin's pI lies on the cathode side of the droplet. Thus, more protein is predicted to be isolated on the cathode side as the field increases. The second observation is that the protein recovery decreased with increasing field strength, presumably as a result of an increasing current. This suggests that significant protein oxidation and/or reduction is occurring as a result of direct contact with the electrodes which renders the protein undetectable. In support of this interpretation is data collected where high protein recoveries were observed (>95%) when isolating the electrodes to reservoirs separated from the drop by dialysis membranes.

To construct an appropriate model of myoglobin focusing in a drop numerical values are substituted into Eq (1). The ratio of ρ/D, defined as α, can be determined by rearranging Eq (2) and using experimental data to solve:

$$\alpha=\frac{\rho}{D}=\frac{1}{Ex_{\sigma}{}^{2}} \tag{3}$$

Previously, myoglobin focused into a band with a standard deviation of 0.6 cm in a 40 cm capillary while applying 10 kV.[39] Thus, when the separation length is 40 cm then α=0.01 V^{-1} cm^{-1} for myoglobin. In the case of a 1.5 cm drop using the same ampholyte mixture, α=0.27 V^{-1} cm^{-1} since ρ is 27 times greater due to the different length scales (40 cm to 1.5 cm) and noting the D is unchanged. Substituting α and x_{pI} into Eq (1) and normalizing the function so the peak area is 1 gives the following relation:

$$C(x)=\sqrt{\frac{0.27E}{2\pi}}e^{\frac{-\left(0.27E(x-0.9)^{2}\right)}{2}} \tag{4}$$

Plots of the model presented in Eq (4) at various field strengths provide a quantitative sense of the expected steady state distributions of myoglobin in dIEF (Figure 4). The relative extent of protein isolation is determined by integrating Eq (4) with respect to the split position and infinity. Splitting the drop at x=0.7 cm results in 59–65% of myoglobin being isolated to the cathode droplet when the electric field is 4–13 V/cm. Thus, the model is consistent with the experimental results collected at equivalent field strengths (Table 1). Although the model is expected to be more accurate with narrowing bandwidth (finite size effects), the differences between the experimental and theoretical findings are attributed to the limited precision (~10% RSD) of the drop splitting mechanism. This along with evaporative and redox effects makes it difficult to assess the model's accuracy from the experimental results alone. Nonetheless, the results suggest that dIEF approaches a steady state, under the conditions employed, similar to that predicted from 1D theory. Furthermore, this simple model can be used to make predictions for other proteins with known α and x_{pI} values.

To improve the separation efficiency of a particular protein either the electric field could be increased or the drop could be split further away from its pI. For example, when 300 V/cm is applied (more typical of electrokinetic techniques) Eq (4) predicts myoglobin would be 99.5% isolated to the cathode droplet when split at the same position (0.7 cm). Experimentally, fields greater than 15 V/cm were not applied since high currents and excessive bubbling occurred. Electrodes can be isolated to separate reservoirs to minimize these effects as is common practice in traditional electrophoretic techniques, with the caveat that the isolated zones must be relatively small volume and the electrodes a short diffusional/transport distance from the separations drop. On the other hand, when splitting the drop at x=0.3 cm while applying a low field strength (13 V/cm) 95% of myoglobin would be isolated to the cathode droplet. Ultimately, this approach requires precise engineering control over drop splitting and it would reduce the volume which is purified.

Protein Focusing Detected by Light Scattering

Visible, unlabelled proteins such as myoglobin or cytochrome c often are precipitated in dIEF at the necessary concentrations for good visualization. Additionally, it is difficult to image the drop directly due to the non-linear optical reflective and refractive effects resulting from the drop's curved surface. Therefore, light scattering was used to provide more direct characterization of protein focusing in dIEF, where the signal is due to

aggregation of the target protein when the local concentration is very high. In these experiments a light-scattering probe, containing optical fibers to deliver light from source and to detector, was scanned across the drop. For simplicity and speed, a smaller drop was used (50 μL and 5 mm length) and the SHS was removed allowing the drop to be suspended in the air.

When a voltage is applied to a drop containing protein an intense scattering signal near 2.75 mm was observed after 18 minutes in three different trials (Figure 5a). The scattering signal was roughly 100 times greater than what is expected from the calibration curve generated by protein standards without applying a voltage (data not shown). Considering its magnitude, we interpret this intense response is the result of protein focusing which stimulates aggregation and leads to larger particles scattering more light. Regardless of the exact mechanism, this scattering signal is not observed in control experiments where either the protein or voltage is removed (Figure 5b–c); confirming that it is a direct result of the protein's presence while applying a voltage.

The light scattering data provides direct evidence of protein focusing in dIEF. The consistent observation of a scattering signal near 2.75 mm confirms that myoglobin is focusing near pH 7.2. It is difficult to assess the bandwidth of the focused zone since the scattering signal is a result of protein aggregation and not protein concentration alone. Additionally, this means the timescale for which the signal is observed, requiring time for aggregation, does not necessarily reflect that for actual protein focusing. Although it is difficult to say for certain, the protein achieves a steady-state focus after approximately 10 minutes since this is when the current stabilizes and the pH gradient is fully established (Figure 3c).

Conclusions

A preliminary investigation of isoelectric focusing within a drop is undertaken here in an effort to develop a separation mechanism compatible with digital microfluidics. Through electrolysis and the use of ampholyte buffers we demonstrate that stable pH gradients can be generated in drops on the order of 10 minutes. Furthermore, light scattering data provides evidence that proteins focus about their pI within the established pH gradient as expected. Combining protein focusing with drop splitting leads to a mechanism for preparative separation. Characterizations using myoglobin reveal that differential protein concentrations are sustained after drop splitting, up to 70%:30% with an electric field of 13 V/cm and by splitting near its pI. These results are found to correlate well to predictions based on quantitative modeling of IEF theory suggesting that dIEF is well behaved and reaches a steady state. Ultimately, these results support the idea that dIEF can be used for purifying protein samples upwards of 99% and that it can be integrated into digital microfluidic systems. This could also be very useful in container less processing of materials in space.

Acknowledgments

RRA and AAG wish to acknowledge funding support provided by NSF CBET0925100. MAH acknowledges support in part with NIH grants 2RO1EB004761-06 and R21EB010191-01A1. Mr. Jim King's help at the NASA John H. Glenn Research Center in setting up the light scattering experiment is very much appreciated. RRA wishes to thank the Research and Technology Division of NASA Glenn Research Center for laboratory support.

References

1. Cesaro-Tadic S, Dermick G, Juncker D, Bourman G, Kropshofer H, Michel B, Fattinger C, Delamarche E. Lab Chip. 2004; 4:563–569. [PubMed: 15570366]
2. Blazej RG, Kumaresan P, Mathies RA. PNAS. 2006; 103:7240–7245. [PubMed: 16648246]
3. Fu J, Schoch RB, Stevens AL, Tannenbaum SR, Han J. Nature Nanotechnology. 2007; 2:121–128.

4. Srisa-Art M, Dyson EC, deMello AJ, Ede JB. Anal Chem. 2008; 80:7063–7067. [PubMed: 18712935]
5. Unger MA, Chou HP, Thorsen T, Scherer A, Quake SR. Science. 2000; 288:113–116. [PubMed: 10753110]
6. Srinivasan V, Pamula VK, Fair RB. Lab Chip. 2004; 4:310–315. [PubMed: 15269796]
7. Teh SY, Lin R, Hung LH, Lee AP. Lab Chip. 2008; 8:198–220. [PubMed: 18231657]
8. Fair RB. Microfluid nanofluid. 2007; 3:245–281.
9. Cho SK, Zhao Y, Jin C, Kim C. Lab Chip. 2007; 7:490–498. [PubMed: 17389966]
10. Fan SK, Huang PW, Wang TT, Peng YH. Lab Chip. 2008; 8:1325–1331. [PubMed: 18651075]
11. Zhao Y, Yi UC, Cho SK. J Microelectromech Syst. 2007; 6:1472–1481.
12. Sista RS, Eckhardt AE, Srinivasan V, Pollack MG, Palanki S, Pamula VK. Lab Chip. 2008; 8:2188–2196. [PubMed: 19023486]
13. Wang Y, Zhao Y, Cho SK. J Micromech Microeng. 2007; 17:2148–2156.
14. Wheeler AR, Jebrail MJ. Anal Chem. 2009; 81:330–335. [PubMed: 19117460]
15. Abdelgawad M, Watson MWL, Wheeler AR. Lab Chip. 2009; 9:1046–1051. [PubMed: 19350085]
16. Schneider J, Egatz-Gomez A, Melle S, Lindsay SA, Dominguez-Garcia P, Rubio MA, Marquez M, Garcia AA. Colloids and Surfaces A. 2008; 323:19–27.
17. Righetti P, Drysdale J. J Chromatogr. 1974; 98:271–321. [PubMed: 4137733]
18. Rodriguez-Diaz R, Wehr T, Zhu M. Electrophoresis. 1997; 18:2134–2144. [PubMed: 9456028]
19. Svensson H. Acta Chem Scand. 1961; 15:325–341.
20. Chu, B. Laser Light Scattering: Basic Principles and Practice. Academic Press; New York: 1991.
21. Ansari RR. J Biomed Optics. 2004; 9:22–37.
22. Egatz-Gomez A, Melle S, Garcia AA, Lindsay SA, Marquez M, Dominguez-Garcia P, Rubio MA, Picraux ST, Taraci JL, Clement T, Yang D, Hayes M, Gust D. Applied Physics Letters. 2006; 89:034106.
23. Garcia AA, Egatz-Gomez A, Lindsay SA, Dominguez-Garcia P, Melle S, Marquez M, Rubio MA, Picraux ST, Yang D, Aella P, Hayes MA, Gust D, Loyprasert S, Vazquez-Alvarez T, Wang J. Journal of Magnetism and Magnetic Materials. 2007:311.
24. Lindsay SA, Vazquez-Alvarez T, Egatz-Gomez A, Loyprasert S, Garcia AA, Wang J. Analyst. 2007; 132:412–416. [PubMed: 17471386]
25. McLauchlin ML, Yang D, Aella P, Garcia AA, Picraux ST, Hayes MA. Langmuir. 2007; 23:4871–4877. [PubMed: 17381139]
26. Li X-M, Reinhoudt D, Crego-Calama M. Chem Soc Rev. 2007; 36
27. Roach P, Shirtcliffe NJ, Newton MI. Soft Matter. 2008; 4
28. Erbil HY, Demirel AL, Avci Y, Mert O. Science. 2003; 299:1377–1380. [PubMed: 12610300]
29. Lu X, Zhang C, Han Y. Macromolecular Rapid Communications. 2004; 25:1606–1610.
30. Ansari RR, Suh KI, Arabshai A, Wilson W, Bray TL, DeLucas LJ. J Crystal Growth. 1996; 168:216–226.
31. Leung AB, Suh KI, Ansari RR. Appl Opt. 2006; 45:2186–2190. [PubMed: 16607982]
32. Simpanya MF, Ansari RR. J Photochemistry and Photobiology. 2008; 84:1589–1595.
33. Datiles MB, Ansari RR, Suh KI, Vitale S, Reed GF, Zigler JS, Ferris FL. Arch Ophthalmol. 2008:126.
34. Macounova K, Cabrera CR, Holl MR, Yager P. Anal Chem. 2000; 72:3745–3751. [PubMed: 10959958]
35. Cabrera CR, Finlayson B, Yager P. Anal Chem. 2001; 73:658–666. [PubMed: 11217778]
36. Klimov A, Pollack GH. Langmuir. 2007; 23:11890–11895. [PubMed: 17939693]
37. Mosher RA, Thormann W. Electrophoresis. 1990; 11:717–723. [PubMed: 2257843]
38. Sebastiano R, Simo C, Mendieta ME, Antonioli P, Citterio A, Cifuentes A, Peltre G, Righetti P. Electrophoresis. 2006; 27:3919. [PubMed: 16991205]
39. Weiss NG, Zwick NL, Hayes M. Journal of Chromatography A. 2010; 1217:179–182. [PubMed: 19945710]

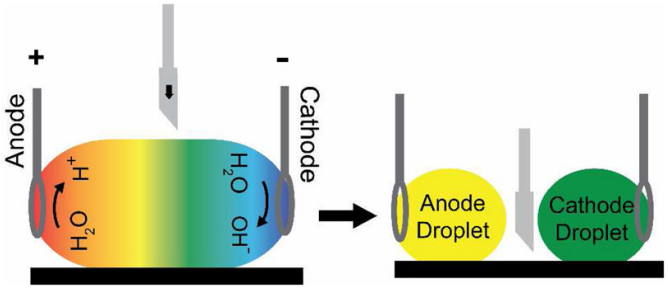

Figure 1.
Schematic illustration of dIEF showing an allantoidal drop supported on a superhydrophobic substrate and pinned between two loop electrodes. Upon applying a voltage the electrolysis of water produces H^+ and OH^- at the anode and cathode, respectively. The transport of these ions can generate a stable pH gradient as illustrated by the color gradient. Then the drop is split by lowering a superhydrophobic 'guillotine' to generate two new drops.

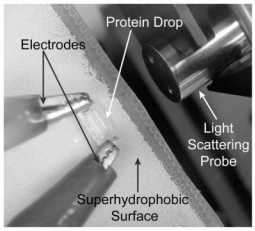

Figure 2.
Setup used for light scattering detection described in experimental section.

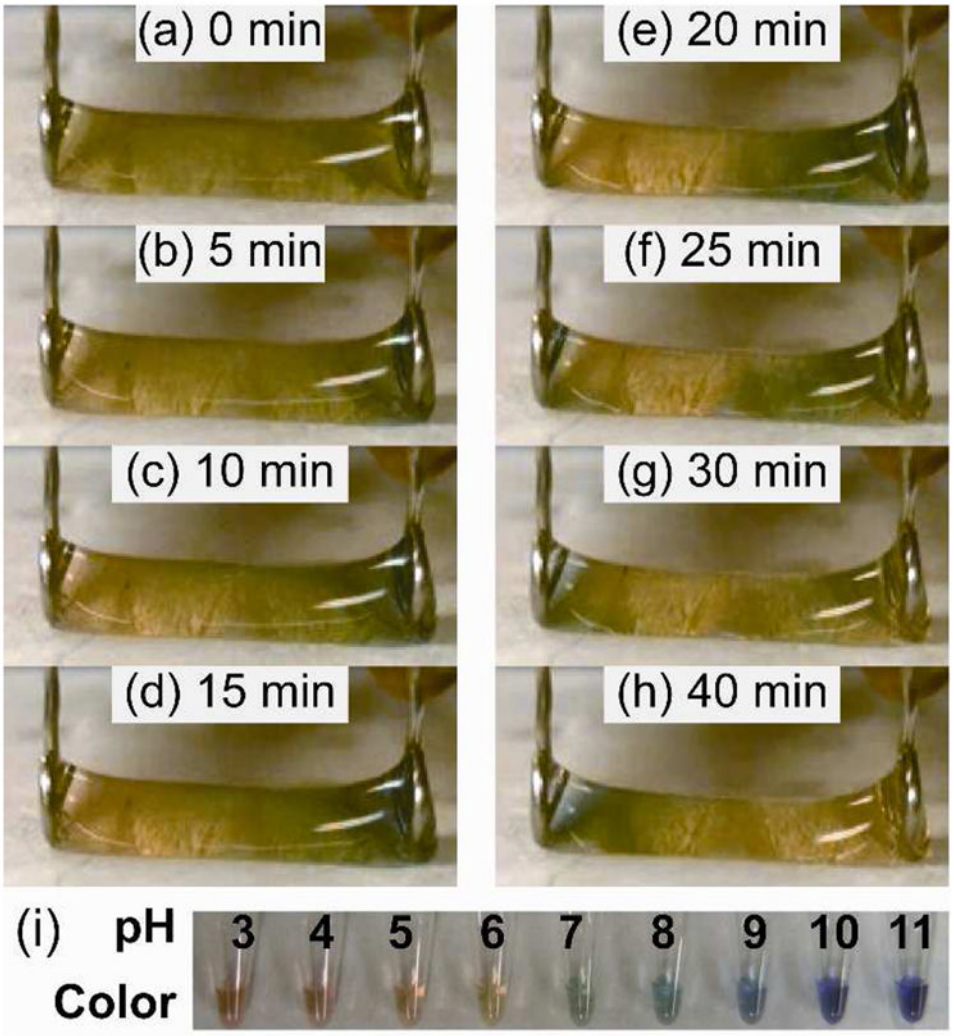

Figure 3.
(a–d) Still images over time showing the generation of a stable pH gradient using 2% pharmalyte 3–10 as the buffer. (e–h) The polarity of the electrodes is switched at t=15 min causing a reversal of the pH gradient. (i) Reference pH solutions and their corresponding color response.

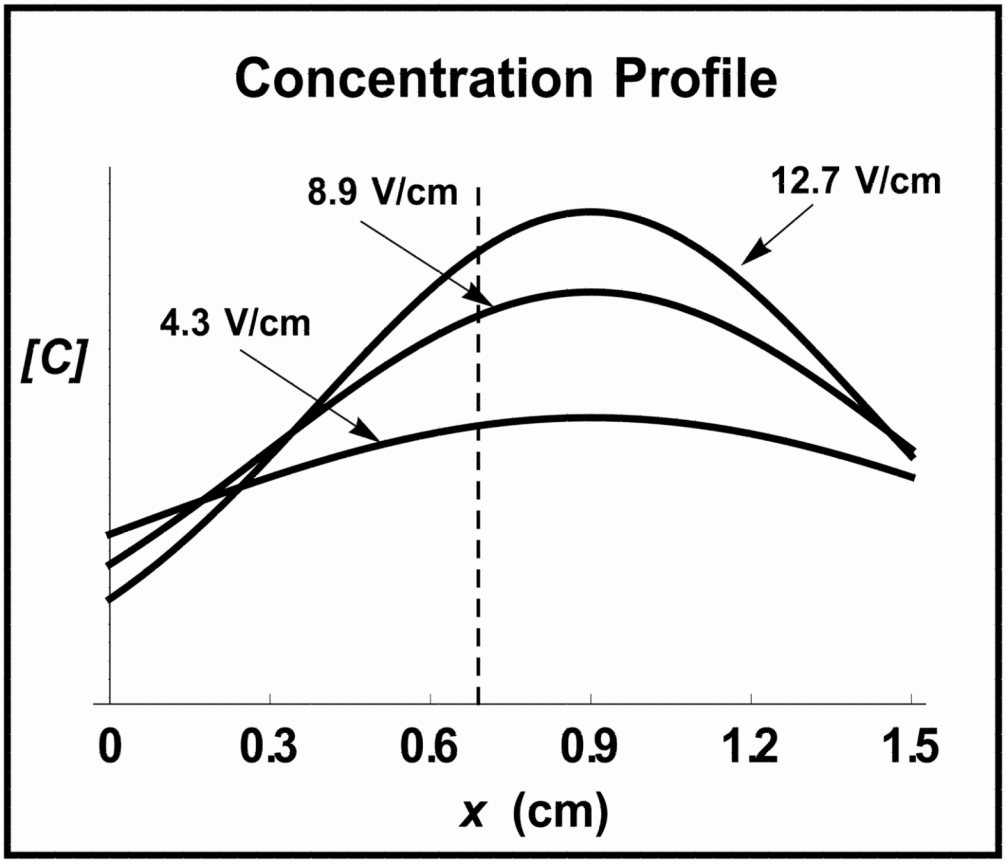

Figure 4.
Concentration profiles of myoglobin focusing in dIEF at different field strengths (Eq 4). Dashed line indicates position where drop was split (0.7 cm).

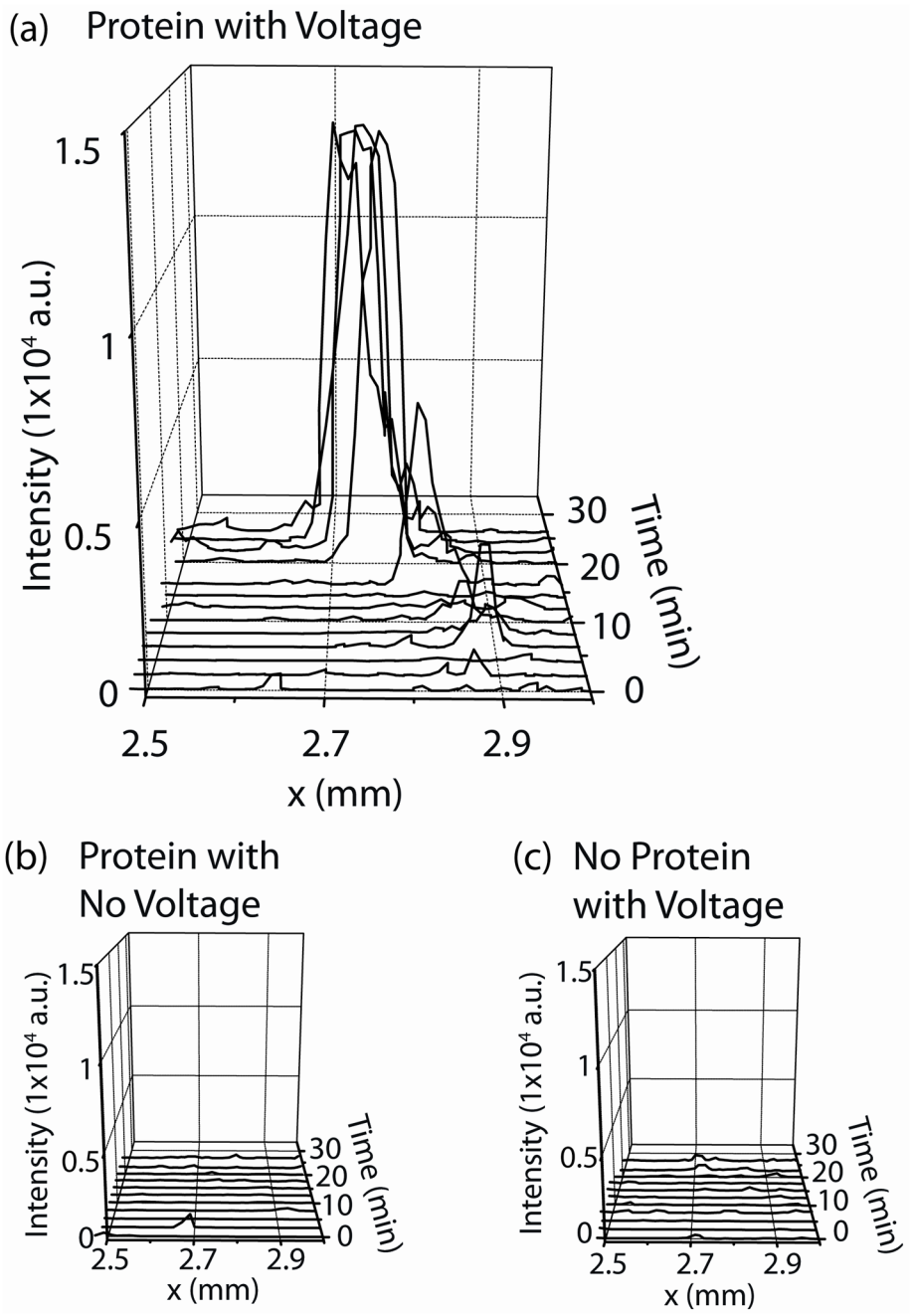

Figure 5.
Whole drop light scattering detection scans taken in 2.5 minute intervals (a) applying voltage to drop containing protein, (b) control experiment where protein is present without voltage, and (c) control experiment where voltage is applied without the protein's presence.

Table 1

Experimental and theoretical findings for myoglobin at various electric fields in dIEF.

Electric Field (V/cm)	Experimental: Relative Myoglobin Mass		Theoretical: Relative Myoglobin Mass		% Recovery
	Anode	*Cathode*	*Anode*	*Cathode*	
4.3	42%	58%	41%	59%	77%
8.9	40%	60%	38%	62%	70%
12.7	28%	72%	35%	65%	65%

Langmuir. Author manuscript; available in PMC 2012 January 4.